OVERVIEW ON SELF-HEALING BOLTED JOINT USING SHAPE MEMORY ALLOYS

Cassio T. Faria, cassiofar@dem.feis.unesp.br
Vicente Lopes Jr., vicente@dem.feis.unesp.br
Grupo de Materiais e Sistemas Inteligentes – UNESP – Faculdade de Engenharia de Ilha Solteira, Avenida Brasil, 56, Ilha Solteira, SP 15385-000.

Daniel J. Inman, dinman@vt.edu
Center for Intelligent Materials Systems and Structures, 310 Durham Hall, Virginia Polytechnic Institute and State University, Blacksburg, VA 24061-0161.

Abstract. *Bolted joints are a mechanical coupling largely used in machinery due its reliability and low cost. The failure of such structure can imply great catastrophes, such as leaking, trains derailment, plane crashes and more. Most of these failures occur due the reduction of the preload, induced by mechanical vibration or human errors on the assembly. This paper is addressed to a overview on application of shape memory alloys (SMA) washers as an actuator to increase the preload on loosed bolted joints. The application of SMA washer is usually followed by a structural health monitoring (SHM) system to identify the damage. Once that changes in structural parameters are significant, a control action goes on, restoring the preload on the joint with the SMA actuator.*

Keywords: *Self-Healing Bolted Joint; SHM; shape Memory Alloy*

1. INTRODUCTION

Bolted joints are one of the most common elements in construction and machine design. They consist of cap screws or studs that capture and join other parts, and are secured with the mating of screw threads. The clamp load, also called preload, of a cap screw is created when a torque is applied, and is generally a percentage of the cap screw's proof strength. Cap screws are manufactured to various standards that define, among other things, their strength and clamp load. Torque charts are available that identify the required torque for cap screws based on their property class.

When a cap screw is tightened it is stretched, and the parts that are captured are compressed. The result is a spring-like assembly. External forces are designed to act on the parts that have been compressed, and not on the cap screw. The result is a non-intuitive distribution of strain; in this engineering model, as long as the forces acting on the compressed parts do not exceed the clamp load, the cap screw doesn't see any increased load.

Bolted joints are largely used in the mechanical systems, due its reliability and low cost, but these discontinuities in the structure are the most common failure sources, is estimated that 70% of all mechanical failure are due fastener failure (Simmons, 1986), requiring huge maintenance efforts to increase structure lifetime. The main maintenance problems related to these bolted joints are the huge number of joints to be inspected and accessibility of some joints, resulting in high costs.

During the past few years, the National Transportation Safety Board (NTSB), an independent U.S Federal government agency, has reported several derailment accidents, most of then caused by failures in the railroad maintenance. As an example, the derailment of Amtrak Train No. 58, shown in figure 1, near Flora, Mississippi in April 6 of 2004, was caused by the lack of maintenance in the joints of the railroad (NTSB, 2005), resulting in 43 injured persons and over 6.8 millions dollars in damages.

Figure 1. Derailment caused by failure on bolted joints

Several other accidents were caused by loose bolted joint, mainly in airplanes, were this kind of failures leads to a catastrophic accident. In June 2008 a Piper PA-34-200T Seneca II crashed in the Manchester International Airport after a failure in the left main landing gear attachments due a loose bolt in this device (AAIB, 2008).

Among several techniques to investigate changes in the structure and relate them to a mechanical failure, one of the most interesting is the impedance-based structural health monitoring (SHM), which relate the electrical impedance of a piezoelectric material attached to a structure, with the mechanical impedance of the structure itself (Lopes Junior, et al, 2000). By comparing the impedance signal of the healthy structure with the real-time signal, one can calculate a damage index, to characterize the structure as healthy or damaged.

When damage is identified, two courses of action can be taken: alert a maintenance team to repair the structure or activate a self-repairing mechanism. This paper will deal with a specific self-repairing mechanism, a shape memory alloy (SMA) washer applied in loosed bolted joints to recover the initial pre-load.

2. IMPEDANCE-BASED SHM

The frequency range used to identify damages has great influence on the results and applicability of the different methods. The advantage in using low frequency measurements is that the modes are global and the sensors can be placed away from the damage locations. However, in this case it requires a significant change in the response, and incipient or specific damages placed in position with low transmissibility cannot be identified. Then, the interpretation of vibration signals to identify damage is not an easy and straightforward task, since always there will be error in the modeling and measurement data. In this context, smart material technology has become an area of increasing interest, and the electrical impedance technique has been accepted as an effective method for structural health monitoring because its easy implementation and simple structural evaluation.

Some of the attributes, which have made piezoelectric actuators particularly attractive for active control, include the large useful bandwidth, the efficient conversion of electrical to mechanical energy, the ability to perform shape control, and the mechanical simplicity of the actuator.

Actuator and sensor can be combined into a single piezoelectric element, called a self-sensing actuator. Self-sensing actuator has a number of desirable properties, related to collocated control, not easily achieved with a separated piezoelectric sensor and actuator. The actuator is typically part of a structure, and the stress, strain, electric field, and electric displacement within a piezoelectric material can be fully described by a pair of electromechanical equations. A piezoceramic (PZT) exhibits a bi-directional effect. Piezoelectricity describes the phenomenon of the generation of an electric field in a material when submitted to a mechanical stress. Stress, strain, and electric displacement within a piezoelectric material can be described by.

$$\{T\} = \left[c^E\right]\{S\} - [e]\{E\} \tag{1}$$

$$\{D\} = [e]^T\{S\} + \left[\varepsilon^S\right]\{E\} \tag{2}$$

where the superscript $(\ )^S$ means that the values are measured at constant strain and the superscript, $(\ )^E$ means that the values are measured at constant electric field, {T} is the stress tensor [N/m^2], {D} is the electric displacement vector [C/m^2], {S} is the strain tensor [m/m], {E} is the electric field [V/m = N/C], [C^E] is the elasticity tensor at constant electric field [N/m^2], [e] is the dielectric permittivity tensor [N.m/V.m^2 = C/m^2], and [ε^S] is the dielectric tensor at constant mechanical strain (permitivity matrix) [N.m/V^2.m]. The letters in brackets indicate the units of the variables (in the SI system of units) with N, m, V, and C denoting Newton, meter, Volts, and Coulomb, respectively.

The electrical impedance is defined as the ratio of the input voltage to the resulting current, while mechanical impedance is defined as the ratio of applied force to the resulting velocity. Electromechanical transducer material, as a piezoelectric provides a means of coupling the mechanical and electrical impedance. Since it is easier to measure electrical impedance than mechanical impedance, this feature can be utilized with advantages, for many applications, where the FRF could be difficulty obtained. The electrical impedance is measured with commercially available impedance analyzers, and it allows extraction of mechanical impedance information from a purely electrical impedance measurement.

There are several distinct requirements for bonded or embedded piezoceramic material to be reliably applied as self-excitation and self-sensing devices for detection and characterization of damage. The partial differential equations describing the dynamics of a beam with surface bonded piezoceramic patches is determined by Banks, et al. (1996). The solution of the electromechanical equations in the scalar case is the theoretical basis of the self-sensing piezoelectric actuator. The equation of motion for a PZT vibrating in the y-direction may be expressed as:

$$\rho \frac{\partial^2 v}{\partial t^2} = \bar{Y}_{22}^E \frac{\partial^2 v}{\partial y^2} \quad (3)$$

where v is the displacement in the y-direction and ρ is the density of the PZT. Separating the displacement into time and spatial domain and applying the boundary conditions, the above equation can be solved.

$$v = \bar{v}\, e^{i\omega t} = \left(A\sin(k.y) + B\cos(k.y)\right)e^{i\omega t} \quad (4)$$

$$k = \omega^2 \frac{\rho}{\bar{Y}_{22}^E} \quad (5)$$

The output displacement of the PZT actuator, the strain, the stress field, as well as the electric displacement field are then determined. The current flowing in PZT is the time rate of the total electric charge between the two electrodes and it is expressed as:

$$I = \iint_{\sigma} i\omega D_3\, d\sigma \quad (6)$$

where σ is the electrode area. The electrical admittance, inverse of the electrical impedance, is Y=I/V, and after some substitution it can be found.

3. CONCEPTS AND MODELING OF THE SMA WASHER

The ideal behavior of the SMA actuator ring in various stages of loading and unloading is presented in the stress–strain diagram shown in Figure 21. The SMA ring is assumed to be submitted to stresses lower then the critical martensite transformation stress, annealed, cycled and originally in austenite phase when not loaded at state O. Before using the SMA actuator ring in the bolted joint, it is loaded and unloaded along the path OABC. Deformations start with compressing the SMA ring from its undeformed state at O to A (where the transition to martensite starts) and then to B (where the material is fully martensite). By unloading the SMA, it reaches state C (where it remains in martensite phase and has negative residual strain).

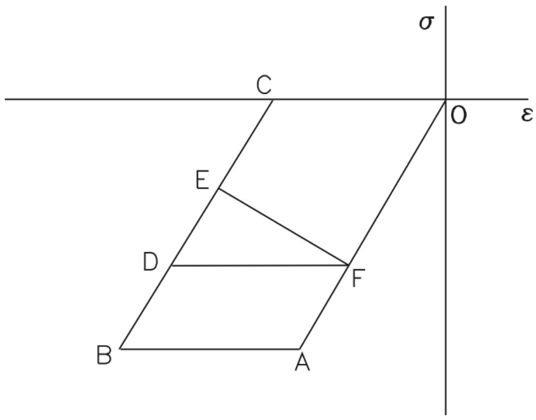

Figure 2. Ideal behavior of the SMA washer.

In any specific bolted joint application, there is an optimal value for the preload. When the actuator ring is used in the bolted joint, the application of this optimal preload imposed to the joint will shift the state of the SMA material from point C to D. Therefore, point D would correspond to the mentioned optimal value of the bolted joint preload. The change from C to D occurs while the material remains totally in the martensite phase.

Now, if for any reason the clamping force in the joint reduces, the SMA state would change to some point E. If E corresponds to a case of too low clamping force, the SMA actuator ring may be activated (by heating) in order to compensate for the lost clamping force in the bolted joint. If it is heated above the austenite finish temperature Af (that itself changes with the applied stress) the complete martensite to austenite transformation occurs. In this way, the Shape Memory Effect occurs and the thickness of the SMA member increases. This increase is required for generating the lost clamping force. Clearly, if the stress level at point D was considered to be optimal, the bolted joint and the actuator ring must be designed in such a way that the final state of the austenite material be at point F with the same stress as point D. As a result, the clamping force corresponding to point F would be essentially the same as the one at point D. In this way, the bolted joint returns to its initial design state that was assumed to be optimal.

In Figure 2 was implicitly assumed that the transformation to martensite (line AB) happens at almost constant stress, at B the transformation to martensite is complete, and during unloading (line BC) no superelasticity occurs. However, actually many transformations are partial and not complete.

Several author modeled the real behavior of these alloys, considering macro and micro variables (Paiva and Savi, 2006). The constitutive equation is basically a function of temperature, stress and strain, the most common way to relate these variables is to created a fourth variable, the martensite fraction. The material law of the SMA in its general form can be written as:

$$\sigma_{SMA} = E(\xi)\varepsilon_{SMA} + \theta\Delta T + \Omega(\xi)\xi \tag{7}$$

where,

$$E(\xi) = (1-\xi)E_A + \xi E_M \tag{8}$$

and

$$\Omega(\xi) = -E(\xi)\varepsilon_L \tag{9}$$

where σ_{SMA} is the stress in the SMA element, ε_{SMA} is the strain in the SMA element, θ is the thermal expansion coefficient, ξ is the martensite fraction, ε_L is the maximum recovery, E_A and E_M are the young modulus for the austenite and martensite phase respectively.

Equation (3) expresses the change in the induced stress in the SMA in terms of corresponding changes in strain, temperature, and the volumetric fraction of martensite in the SMA. Equation (7) is valid for changes between two states. It can express the mechanical behavior of the SMA whether it is undergoing phase transformations or not. Without phase transformations, the last term in this equation vanishes and a simple thermo-elastic equation is obtained. If the process is also isothermal, the change in the temperature would be cancelled as well and equation (7) reduces to Hooke's law. (Brinson, 1993) describes the behavior of the martensite fraction when temperature changes.

For austenite to martensite transformation:

$$\begin{gathered} \xi = \frac{1-\xi_0}{2}\cos\left[a_m\left(T - M_f\right) + b_m\sigma\right] + \frac{1+\xi_0}{2} \\ M_f^{'} < T < M_s^{'} \end{gathered} \tag{10}$$

Where:

$$M_f^{'} = M_f + \frac{\sigma}{C_M}, \quad M_s^{'} = M_s + \frac{\sigma}{C_M} \tag{11}$$

$$a_m = \frac{\pi}{M_s - M_f} \tag{12}$$

$$b_m = \frac{-a_m\left(M_f^{'} - M_f\right)}{\sigma} \tag{13}$$

where M_S and M_f are the initial and final temperature for the transformation austenite to martensite, respectively, C_M is the stress martensite inducer coefficient and ξ_0 the initial martensite fraction in the transformation.

The inverse transformation is described as:

$$\xi = \frac{\xi_0}{2}\left\{\cos\left[a_a\left(T - A_s\right) + b_a\sigma\right] + 1\right\}$$
$$A_s^{'} < T < A_f^{'} \tag{14}$$

Where:

$$A_f^{'} = A_f + \frac{\sigma}{C_A}, \quad A_s^{'} = A_s + \frac{\sigma}{C_A} \tag{15}$$

$$a_a = \frac{\pi}{A_s - A_f} \tag{16}$$

$$b_a = \frac{-a_a\left(A_f^{'} - A_f\right)}{\sigma} \tag{17}$$

where A_S and A_f are the initial and final temperature for the transformation austenite to martensite, respectively and C_A is the stress martensite inducer coefficient.

It is important to notice that the variables of this model are the effective ones, once that the modeling is conceived for a tensile situation. To relate the model to another situation usually von-misses stress and strain are applied, as well as the temperature in Kelvin. The effective stress and strain can be calculated by the following equations:

$$\sigma = \frac{1}{\sqrt{2}}\left[\left(\sigma_z - \sigma_r\right)^2 + \left(\sigma_r - \sigma_\theta\right)^2 + \left(\sigma_z - \sigma_\theta\right)^2\right]^{\frac{1}{2}} \tag{18}$$

$$\varepsilon = \frac{1}{\sqrt{2}}\left[\left(\varepsilon_z - \varepsilon_r\right)^2 + \left(\varepsilon_r - \varepsilon_\theta\right)^2 + \left(\varepsilon_z - \varepsilon_\theta\right)^2\right]^{\frac{1}{2}} \tag{19}$$

The stress is one-dimensional, in Z direction, so equation (18) can be reduced to:

$$\sigma = \left|\sigma_z\right| \tag{20}$$

One can despite the change in the thickness of the SMA washer during its transformation, resulting in a null strain in R direction, then by the constant volume assumption:

$$\varepsilon_z + \varepsilon_\theta = 0 \tag{21}$$

Combining equations (19) and (21) the effective strain applied on the smart material is:

$$\varepsilon = \sqrt{3}\ \left|\varepsilon_z\right| \tag{22}$$

As a result equation (7) can be written as a function of the stress and strain in the Z direction. The linear thermal expansion of the alloy is ignored once that just the full cycle of actuation is important for this application (i.e. after heating and cooling the actuator, the system will achieve a new steady-state pre-load level).

$$\left|\sigma_z\right| = E\left(\xi\right)\sqrt{3}\left|\varepsilon_z\right| - E\left(\xi\right)\varepsilon_L\xi \tag{23}$$

In equation (23) two variables are unknown: the stress and strain in Z direction. In order to solve this problem another equation have to be derivate, one can describe the behavior of the bolted joint when a pre-load is applied, this new equation can be manipulated to also be a function of the stress and strain in the actuation element, the initial idea is to do it considering the joint an elastic element, being the equation a variation of the Hooke's law, as follows:

$$\Delta_{SMA(\varepsilon_Z)} = K_{J+B} \quad \Delta P_{(\sigma_Z)} \tag{24}$$

where Δ_{SMA} is the growth in the axial direction of the SMA washer, K_{J+B} is the equivalent stiffness of the bolted joint and ΔP is the change in the pre-load.

4. SMART JOINT

The initial concept of this device was presented by Haimi, et. al. (1997) that proposed a method for pre-tensioning bolted joints based on a shape memory alloy actuators. The main purpose was to have a shear-less joint. Based on this kind of actuator and in the development of the damage detection technology through the impedance-based method Park and Inman (2001) proposed and tested a smart self-healing bolted joint. The results showed a recovery in the impedance signal of the joint after the SMA actuation.

Park, et. al. (2003) proceeded the investigation in the self-repairing mechanism using shape memory alloys along with a self-sensing mechanism using piezoelectric elements to measure the electrical impedance and relate it to the mechanical one, figure 3 illustrate this procedure.

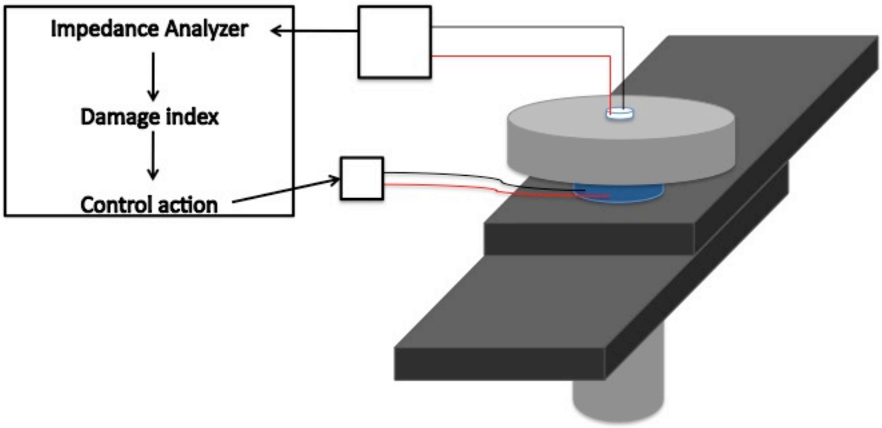

Figure 3. Schematics of the self-healing bolted joint using a PZT sensing element and a SMA actuator.

Peairs, et. al. (2004) investigate some practical issues of this technique, comparing the heating of the actuator through two different methods, with an external heater and a resistive heating, basically the first one has a better energy efficiency and a more compact setup is needed for actuation.

Due the lack of information on the compression behavior of SMA actuators Hesse, et. al. (2004) carried out a complete investigation and characterization of the SMA elements in compression comparing with the tensile data, also a direct measurement of the clamping force in the joint were done. As a sequence for this journal article Ghorashi, et. al. (2004) presented a mathematical modeling for the self-healing process. Antonios, et. al. (2006) redid the experimental and numerical analysis for the self-healing bolted joint, studding the influence of some aspects, such as: initial clamping force, heating and cooling rate, heat loss for different insulation materials and the analytical modeling.

Kim, et. al. (2009) proposes a digital impedance-based SHM, this concept eliminates A/D and D/A convertors, being a more compact SHM analysis setup, another important contribution is the development of a graphic user interface that allows the user to change the baseline, define a threshold for the damage situation and choose the analyzed frequency range.

5. CONCLUSIONS

The present contribution discusses main aspects of a self-sensing and self-healing bolted joint using a shape memory alloy element as the actuator to regain the clamping. A change in the SMA tensile model is proposed in order to describe its behavior in compression. Also an impedance based structural health monitoring mathematical modeling is presented for piezoelectric sensing elements.

6. ACKNOWLEDGEMENTS

The authors gratefully acknowledge the support of the Association of American Railroads and the Railway Technology Laboratory at Virginia Tech.

7. REFERENCES

AAIB. Accident Report of Piper PA-34-200T Seneca II, G-JDBC, June 2008 in Manchester International Airport. Manchester 2008.

Antonios, C., D. J. Inman, et al. Experimental and Theoretical Behavior of Self-healing Bolted Joints. Journal of Intelligent Material Systems and Structures, v.17, n.6, June 1, 2006, p.499-509. 2006.

Banks, H. T., D. J. Inman, et al. AN EXPERIMENTALLY VALIDATED DAMAGE DETECTION THEORY IN SMART STRUCTURES. Journal of Sound and Vibration, v.191, n.5, p.859-880. 1996.

Brinson, L.C., "One Dimensional Constitutive Behavior of Shape Memory Alloys: Themomechanical Derivation with Non Constant Material Functions and Redefined Martensite Internal Variable", Journal of Intelligent Material Systems and Structures, n. 4, pp. 229-242, 1993.

Ghorashi, M. e D. J. Inman. Shape Memory Alloy in Tension and Compression and its Application as Clamping Force Actuator in a Bolted Joint: Part 2 -- Modeling. Journal of Intelligent Material Systems and Structures, v.15, n.8, August 1, 2004, p.589-600. 2004.

Haimi, E., J. Keto-Tokol, et al. A Method for Pre-Tensioning of Bolts Based On Shape Memory Alloy Actuators and Active Heating. Second International Conference on Shape Memory and Superelastic Technologies. Pacific Grove - CA - USA, 1997. 275-280 p.

Hesse, T., M. Ghorashi, et al. Shape Memory Alloy in Tension and Compression and its Application as Clamping-Force Actuator in a Bolted Joint: Part 1 -- Experimentation. Journal of Intelligent Material Systems and Structures, v.15, n.8, August 1, 2004, p.577-587. 2004.

Kim, J. K., D. Zhou, et al. A structural health monitoring system for self-repairing: SPIE, 2009. 729512 p.

Lopes, V., Jr., G. Park, et al. Impedance-Based Structural Health Monitoring with Artificial Neural Networks. Journal of Intelligent Material Systems and Structures, v.11, n.3, March 1, 2000, p.206-214. 2000.

NTSB. Derailment of Amtrak Train No. 58, City of New Orleans, Near Flora, Mississippi, April 6, 2004. Washington, DC. 2005.

Paiva, A. e M. A. Savi. An overview of constitutive models for shape memory alloys. Mathematical Problems in Engineering, v.2006, p.30. 2006.

Park, G. e D. J. Inman. Smart bolts: an example of self-healing structures. Smart Materials Bulletin, v.2001, n.7, p.5-8. 2001.

Park, G., D. Muntges, et al. Self-repairing joints employing shape-memory alloy actuators. JOM Journal of the Minerals, Metals and Materials Society, v.55, n.12, p.33-37. 2003.

Peairs, D. M., G. Park, et al. Practical issues of activating self-repairing bolted joints. Smart Materials and Structures, n.6, p.1414. 2004.

8. RESPONSIBILITY NOTICE

The authors are the only responsible for the printed material included in this paper.